

Influence of ferroptosis indicators on the stability of atherosclerotic plaque

Hong Guo^{1,2}, Aobo Zhang¹, Lei Qiu³, Jianhui Mao², Lei Zheng⁴, Zongmao Zhao^{1*}¹Department of Neurosurgery, The Second Hospital of Hebei Medical University, Shijiazhuang 050000, China²Department of Neurosurgery, Harrison International Peace Hospital, Hebei Medical University, Hengshui 053000, China³Department of Pathology, Harrison International Peace Hospital, Hebei Medical University, Hengshui 053000, China⁴Central Laboratory, Harrison International Peace Hospital, Hebei Medical University, Hengshui 053000, China

ARTICLE INFO

Original paper

Article history:

Received: June 19, 2023

Accepted: November 25, 2023

Published: December 10, 2023

Keywords:

Atherosclerosis, ferroptosis, plaque stability

ABSTRACT

Ferroptosis is a new form of cell death that is unique and closely related to iron concentration, and reactive oxygen species (ROS) production. We investigated the indicators of ferroptosis between vulnerable plaque and stable plaque in atherosclerotic. Quantitative real-time polymerase chain reaction (qRT-PCR) and Western blotting were used to detect the expression of the ferroptosis-related genes and proteins and extracellular matrix stability-related genes and proteins (FN, CoL-1). Superoxide dismutase (SOD) activities, glutathione peroxidase (GSH) and malondialdehyde (MDA) were detected by ELISA. The commercially available kit was used to detect Fe²⁺ concentration in tissue. DCFH-DA fluorescent probe was used to detect the ROS levels. H&E stain, Masson trichrome stain, and Oil Red O stain were used to detect pathological states in vulnerable plaque and stable plaque. Tissue localization and positive rate of GPX4, SLC7A11, COX-2, FN, and COL-1 were evaluated by immunohistochemistry. The results showed a significant increase in the expression of COX2 and a significant decrease in the expression of GPX4 and SLC7A11 in genes related to ferroptosis in vulnerable plaque compared with stable plaque. Pathologic results showed vulnerable plaque with higher levels of inflammatory cell infiltration, more diffuse collagen fibers, and larger particles of lipid droplets. Concentrations of the antioxidant metabolites SOD and GSH were significantly reduced and concentrations of the oxidative metabolites MDA and Fe²⁺ were significantly increased in vulnerable plaque compared with stable plaque. The expression of FN and CoL-1 was significantly reduced in genes related to extracellular matrix stability in vulnerable plaque. Taken together, these findings indicate that the degree of ferroptosis in vulnerable plaque is higher than that in stable plaque, suggesting that changes in indicators of ferroptosis may affect carotid atherosclerotic plaque stability, target spot in the ferroptosis signaling pathway may provide further theoretical basis for the clinical treatment of carotid atherosclerosis.

Doi: <http://dx.doi.org/10.14715/cmb/2023.69.13.31>Copyright: © 2023 by the C.M.B. Association. All rights reserved. 

Introduction

Atherosclerosis (AS) is a disease characterized by arterial stenosis on account of a disorder of lipid metabolism and AS plaque formation in artery walls (1, 2). The leading cause of morbidity and mortality in advanced AS is plaque rupture and subsequent acute cardiovascular complications (3-5). Despite recent advances in primary prevention and treatment techniques, the incidence of the disease continues to rise (6, 7). The direct cause is the rupture of vulnerable plaque, which has a weak fibrous cap and high surface pressure that makes it susceptible to rupture and bleeding (8). Vulnerable plaques are more prone to thrombosis, and a growing body of research suggests that the onset and progression of acute coronary syndromes are more closely related to coronary plaque stability (9, 10). Severe carotid stenosis with vulnerable plaque is an important risk factor for the development of ischemic stroke (11).

Ferroptosis is a new type of cell death characterized by iron-dependent lipid peroxidation and decreased glutathione peroxidase 4 (GPX4) activity, which leads to oxidative stress and cell death (12). The important role of fer-

roptosis in the development of AS has attracted widespread attention (13). Ahluwalia et al. studied the relationship between serum ferritin concentration and carotid atherosclerotic plaques, it found that for every 10 mg/L increase in ferritin concentration, the probability of atherosclerotic plaque formation increased by 3% (14). When there is an excess of free iron in the cell, a large amount of reactive oxygen species (ROS) through the Fenton reaction, accelerating the oxidation of LDL (15). Large amounts of oxidized low-density lipoprotein (OX-LDL) are phagocytosed by macrophages to form foam cells (16). Foam cells upregulate protein hydrolases and degrade extracellular matrix structures, leading to the rupture of coronary atherosclerotic plaques and thus causing acute adverse cardiovascular events (17).

Normally, cells are in a dynamic balance between oxidation and antioxidants. Because of the influence of external factors, there is an increase in oxidized molecules in the organism, such as an increase in the content of ROS. meanwhile, the intracellular antioxidant system is disrupted, such as the reduction of superoxide dismutase (SOD), solute carrier family 7 member 11 (SLC7A11), glutathione peroxidases (GPXs) and glutathione (GSH). The balance

* Corresponding author. Email: zzm692017@sina.com

between oxidation and antioxidants in the organism is disturbed, which leads to the occurrence of ferroptosis (18). The Ferroptosis process further generates large amounts of ROS that increase the level of oxidative stress in the cell, and ROS further promotes cyclooxygenase 2(COX-2) to oxidize the lipids in the cell membrane, generating large amounts of lipid peroxides such as malondialdehyde (MDA) (19). During the process of atherosclerosis, structural stabilization of the extracellular matrix is altered, leading to easier plaque detachment, which may be associated with the genes for extracellular matrix stabilization-related genes, fibronectin 1(FN) and Collagen I(COL-1). FN has an important role in cellular adhesion and is involved in the maintenance of cellular morphology (20), and COL-1 is important in supporting the structure of the extracellular matrix (21). In the progress of Ferroptosis, matrix metalloproteinases (MMPs) are secreted by activated macrophages and degrade extracellular matrix proteins, leading to thinning of the atherosclerotic lipid fibrous cap, increased fragility, and accelerated rupture of atherosclerotic plaques (22, 23).

Vulnerable plaques in patients with atherosclerosis are an important cause of stroke formation, and how to stabilize vulnerable plaques is the key to solving this problem. The mechanism of ferroptosis may play an important role in the formation of vulnerable plaques. Therefore, we explored the mechanism of ferroptosis in atherosclerotic plaques, which may provide ideas for the future development of new drugs to stabilize plaques.

Materials and Methods

Patients

We collected carotid plaque and clinical data from a total of 70 patients who underwent carotid endarterectomy at our hospital between June 2021 and December 2022. According to the histopathological definition and criteria for vulnerable plaques in carotid atherosclerotic plaques developed by the American Heart Association (AHA) in 1995 (24) and Naghavi et al. in 2003 (25). plaques with a large lipid core, thin fibrous cap, intra-plaque hemorrhage and secondary thrombosis were identified as vulnerable plaques. The study was approved by the Ethics Committee of our hospital and all enrolled patients signed an informed consent form.

RT-qPCR

Total RNA was isolated from tissues using TRIzol (Invitrogen, Carlsbad, CA, USA) according to the manu-

facturer's protocol. Purification of RNA was performed strictly according to the instructions of the RNA extraction kit (TaKaRa, Tokyo, Japan). the purity and concentration of RNA were detected by micro-nucleic acid assay (Thermo, Waltham, MA, USA), and cDNA was synthesized in accordance with the reverse transcription kit (TaKaRa, Tokyo, Japan). Primer design was carried out using software Primer 5 (primers for COX-2, GPX4, SLC7A11, FN, CoL-1) (Table 1), and the following conditions were followed Reverse transcription reaction was carried out: 37°C, 30 min; 94°C, 2 min. Add the synthesized primers (Sangon Biotech, Shanghai, China) and perform primer amplification using an RT-PCR kit (TaKaRa, Tokyo, Japan) under the following conditions: pre-denaturation 95°C, 10 min, denaturation 95°C, 10 S, annealing 60°C, 20 S, annealing extension 72°C, 10 min, and amplification for 40 cycles. The number of cycles reaching the threshold (Ct value) in the reaction tube was recorded. The relative expression of each target gene was calculated using the $2^{-\Delta\Delta Ct}$ method and GAPDH was used as the reference.

Western blotting

A small amount of tissue (30-50 mg) block was placed in the homogenizer (Scientz Biotechnology, Ningbo, China) and cut the tissue block with clean scissors, then add 400 μ L RIPA (containing PMSF) (Solarbio, Beijing, China). After 30 min of lysis on ice, the lysate could be pipetted into a 1.5 ml centrifuge tube and then centrifuged at 12,000 rpm for 5 min at 4°C. The supernatant was dispensed into 0.5 ml centrifuge tubes and stored at -20°C. After detecting the protein content, the protein expression of the target proteins COX-2 (Abcam, Cambridge, MA, USA) (1:1000), GPX4 (Abcam, Cambridge, MA, USA) (1:1000), SLC7A11 (Abcam, Cambridge, MA, USA) (1:1000), FN(Abcam, Cambridge, MA, USA) (1:1000), CoL-1 (Abcam, Cambridge, MA, USA) (1:1000) was detected according to the steps of SDS-PAGE electrophoresis, membrane transfer, sequential incubation of primary antibody and secondary antibody, chemiluminescence and fixation.

ELISA

Plaque cells were disrupted by repeated grinding, centrifuged for 20 minutes (2000-3000 rpm) and the supernatant was collected. Dilution of standards, the addition of samples, warming, preparation, washing, the addition of enzyme reagents, color development, termination of the reaction and assay were carried out according to the protocol of the SOD, GSH and MDA ELISA kit (Solarbio,

Table 1. Oligonucleotide sequences used for real-time polymerase chain reaction.

Primer sequence	
GPX4	F: 5'-GGGCTACAACGTCAAATTCG-3'
	R: 5'-TCCACTTGATGGCATTTC-3'
SLC7A11	F: 5'-TTCAATCCCCTTCTCCACCTAA-3'
	R: 5'-CTTCATTCCATCTTCATAATAACCCTGT-3'
COX2	F:5'-TGCCGTGGTTTCCGTTGCTTG-3'
	R:5'-TCACATTTGATGGTCGTCTTGTCGTCT-3'
FN	F: 5'-ATGCGCTAGCGATCGATAGCTAGCTAGC-3'
	R: 5'-GCTACGCTAGCTAGCTACAGCTACGCAA-3'
COL-1	F:5'-GATCAGCTAGCTAGCATGCAGTCACTCGA-3'
	R:5'-CGTAGTCGACGATCGACTCGACGCTACGA-3'

Beijing, China). It is noted that the washing process should be repeated 5 times.

Detection of ROS by flow cytometry

DCFH-DA is a probe for the detection of intracellular ROS. DCFH-DA working solution was prepared, and plaque tissues were digested, collected and stained. After adding 1 mL of 1×DCFH-DA working solution (DOJINDO, Kumamoto, Japan) and incubating for 30 min, the cells were washed and resuspended with PBS and then analyzed for ROS concentration by flow cytometer.

Fe²⁺ level detection

Plaque tissue was sheared and digested with trypsin into a cell suspension, centrifuged and the supernatant discarded. Add 0.9 mL of buffer per 1 million cells. The cells were broken by ultrasound (Scientz Biotechnology, Ningbo, China) (power 200 W, ultrasound 3 s, interval 10 s, repeat 30 times), and centrifuged at 10,000 g 4°C for 10 min. The supernatant was taken and the OD value was measured at 593 nm according to the instructions of the Fe²⁺ detection kit (Abcam, Cambridge, MA, USA).

H&E stain

The specimens were fixed by formalin solution and dehydrated by gradient alcohol. After paraffin embedding, the specimens were sliced up and the thickness of the slices was 5 μm. The prepared slices were heated in the oven at 60°C for 2 h. The slices were removed from the oven and cooled at room temperature before dewaxing and dehydration. Hematoxylin and 0.5% eosin staining were performed, followed by washing, dehydration and air drying. Neutral gum was added dropwise, then coverslips were sealed. The slices were observed under the microscope and five random fields of view were collected.

Masson trichrome stain

The slices were stained with Weigert's iron hematoxylin in Masson's staining kit for 5 min and acidic magenta for 5-10 min. The slices were then treated with aqueous phosphomolybdic acid for about 3-5 min and stained with aniline blue for 5 min. After dehydration and sealing of the slices, the slices were viewed under a microscope and the images were collected. Collagen fibers, mucus and cartilage were stained blue; muscle fibers, fibrin and erythrocytes were stained red; and cell nuclei were stained blue-black.

Oil red O stain

Human carotid artery tissues were placed in a quick-freezing tank with peripheral drops of embedding agent, and frozen at -25°C for 30 minutes. Then frozen sections were performed, and the thickness of the sections was 6-10 μm. 4% paraformaldehyde was dripped on the tissue sections to fix them for 10 minutes, and 60% isopropanol was used for rinsing after washing with distilled water. Oil red o staining solution was stained for 10 minutes and then rinsed using 60% isopropanol and distilled water respectively. Hematoxylin staining for 3-5 minutes, distilled water rinsing 3 times, using glycerol gelatin to seal the film, 4°C storage spare. The staining of human carotid artery tissues in each group was observed under a light microscope and photographed.

Immunohistochemistry

The atheromatous plaques were put into 10% neutral formalin for internal fixation, subjected to gradient alcohol dehydration, embedded in wax blocks and sectioned in a microtome (Leica, Wetzlar, Germany). Subsequently, wax blocks were dewaxed separately, antigen repair was performed using sodium citrate, goat serum was closed and incubated overnight at 4°C using the following primary antibodies: GPX4 (Abcam, ab125066, Cambridge, MA, USA), SLC7A11 (Abcam, ab37185, Cambridge, MA, USA), COX-2 (Abcam, ab16701, Cambridge, MA, USA), FN (Abcam, ab2413, Cambridge, MA, USA), COL-1 (Abcam, ab138492, Cambridge, MA, USA), washed and then incubated with the secondary antibodies for 30 minutes Goat Anti-Rabbit IgG (Abcam, ab6721, Cambridge, MA, USA), Goat Anti-Mouse IgG (Abcam, ab6728, Cambridge, MA, USA). The staining reaction was then carried out using DAB (Solarbio, Beijing, China), and hematoxylin (Solarbio, Beijing, China). Stained paraffin sections were photographed under a light microscope (Olympus, Tokyo, Japan), 5 random fields of view were selected for each sample picking and the average optical density of the sections was analyzed semi-quantitatively using ImageJ software.

Statistical analysis

All experiments were repeated at least 3 times independently and all data were expressed as mean ± standard deviation (mean ± SD). Gray scale analysis of Western Blot strips was performed by ImageJ software. The data were analyzed by Statistic Package for Social Science (SPSS) 22.0 (IBM, Armonk, NY, USA), and the representative graphs were created by GraphPad Prism 5 (La Jolla, CA, USA). Comparisons between groups were made by t-test and one-way ANOVA.

Results

Difference between vulnerable plaque and stable plaque

Plaques isolated by carotid endarterectomy show that vulnerable plaques typically have large lipid cores, thin fibrous caps, intra-plaque hemorrhage, and secondary thrombosis (Figure 1). The plaques were classified into vulnerable plaques (31 cases) and stable plaques (39 cases) based on appearance and pathology. Age, gender, carotid stenosis and operative side of the patients were counted separately as shown in Table 2.

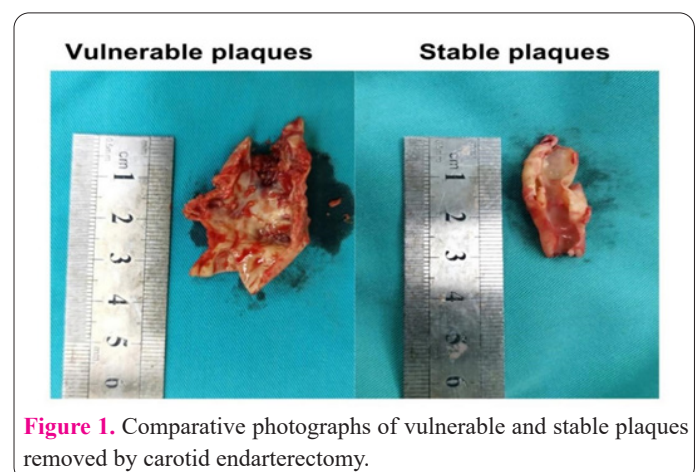


Figure 1. Comparative photographs of vulnerable and stable plaques removed by carotid endarterectomy.

Table 2. Statistics between carotid plaques and clinical characteristics of patients.

Clinicopathological variables		Vulnerable plaques (n=31)	Stable plaques (n=39)
Age(yr)		68.94(6.24)	69.23(7.20)
Gender	Female	6	12
	Male	25	27
carotid stenosis	≥70%	23	29
	>50% and <70%	8	10
operative side	Left	13	20
	Right	18	19

The degree of ferroptosis and extracellular matrix instability

The degree of ferroptosis and extracellular matrix instability were higher in vulnerable plaques than in stable plaques at the protein and mRNA expression levels.

To verify the degree of ferroptosis and extracellular matrix stability in vulnerable plaques and stable plaques, we measured the protein and mRNA of the ferroptosis pathway and extracellular matrix instability. As shown in Figure 2A-B, the expression levels of GPX4 and SLC7A11 were significantly higher in stable plaques than the vulnerable plaques. The expression level of COX-2 was significantly lower in in stable plaques than the vulnerable plaques. Compared with the vulnerable plaques, the expression of FN and COL-1 related to maintaining the stability of the extracellular matrix was significantly higher.

Levels of vulnerable plaques

Vulnerable plaques had higher levels of lipid peroxidation markers and lower levels of antioxidant factors than

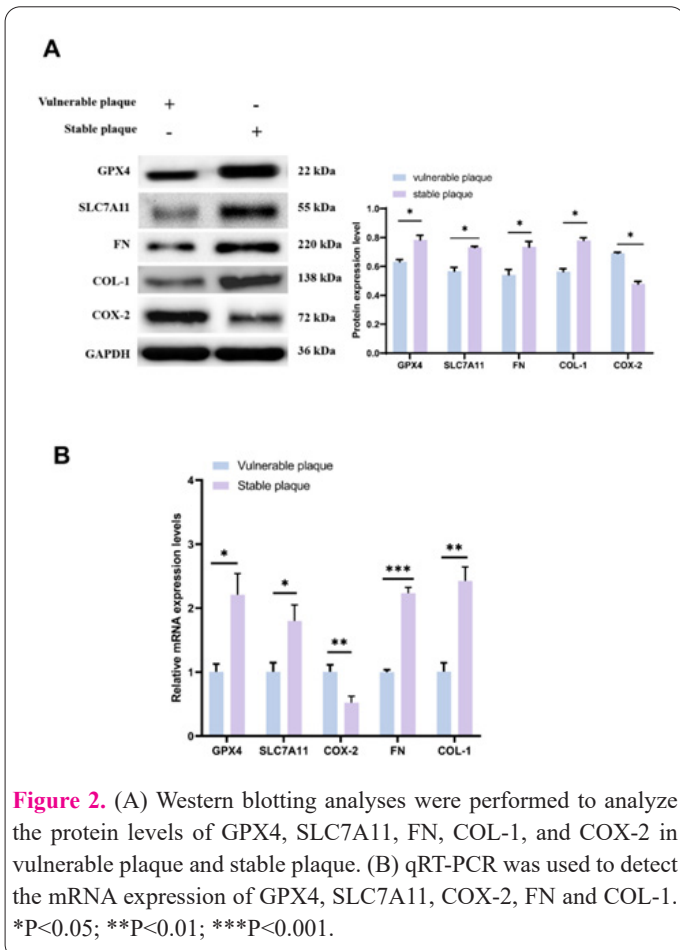


Figure 2. (A) Western blotting analyses were performed to analyze the protein levels of GPX4, SLC7A11, FN, COL-1, and COX-2 in vulnerable plaque and stable plaque. (B) qRT-PCR was used to detect the mRNA expression of GPX4, SLC7A11, COX-2, FN and COL-1. *P<0.05; **P<0.01; ***P<0.001.

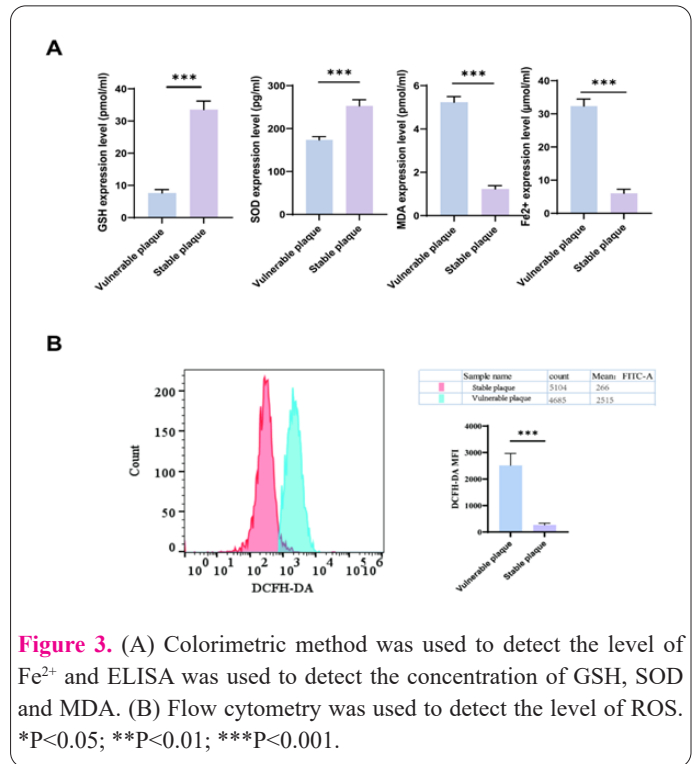


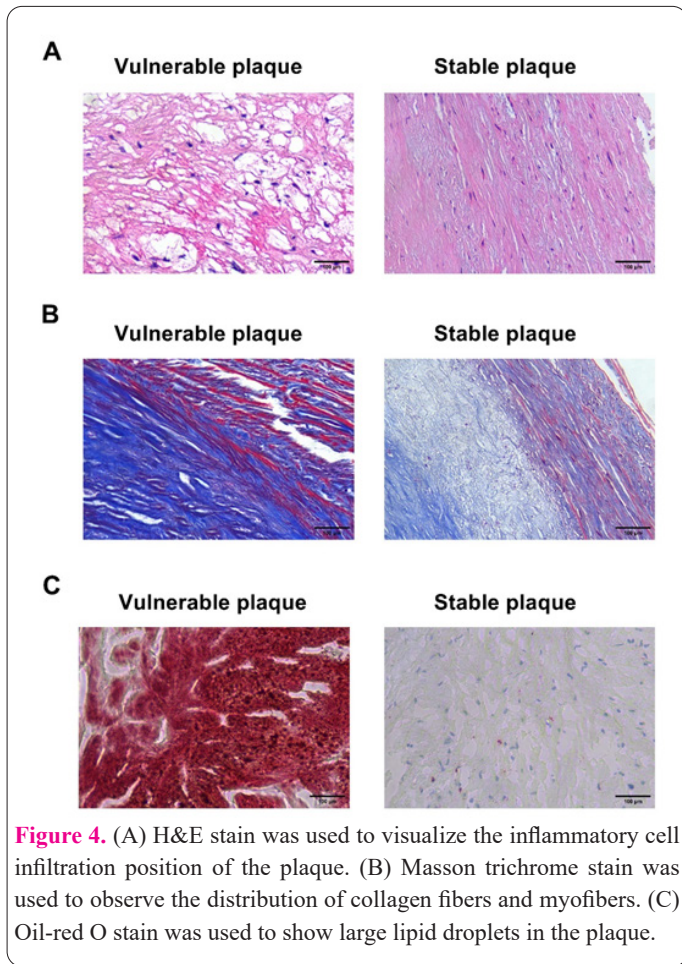
Figure 3. (A) Colorimetric method was used to detect the level of Fe²⁺ and ELISA was used to detect the concentration of GSH, SOD and MDA. (B) Flow cytometry was used to detect the level of ROS. *P<0.05; **P<0.01; ***P<0.001.

stable plaques.

The pathologic features of Ferroptosis are mainly characterized by disorder in iron metabolism and accumulation of lipid peroxides. To detect the state of iron metabolism, we examined the level of Fe²⁺ by colorimetric method, as shown in Figure 3A, the concentration of Fe²⁺ was significantly higher in vulnerable plaques than the stable plaques (P<0.001). We evaluated the concentrations of SOD, GSH and MDA using ELISA, the concentrations of SOD and GSH with antioxidant effects were significantly lower in vulnerable plaques than in stable plaques (P<0.001). Compared with the stable plaques, the concentration of MDA was significantly higher (P<0.001). We detected the level of ROS using flow cytometry, as shown in Figure 3B, the results showed that the level of ROS was significantly higher in the vulnerable plaques than in the stable plaques.

Comparison of pathological staining of vulnerable and stable plaques

HE stain results showed more inflammatory cell infiltration in vulnerable plaque than stable plaque. Masson trichrome stain results showed that the vulnerable plaque had more diffuse collagen fibers. Oil red O stain showed more large lipid droplets in vulnerable plaque than in stable plaque (Figure 4).



The degree of ferroptosis and extracellular matrix instability

The degree of ferroptosis and extracellular matrix instability were higher in vulnerable plaques than in stable plaques in terms of protein localization and quantitation.

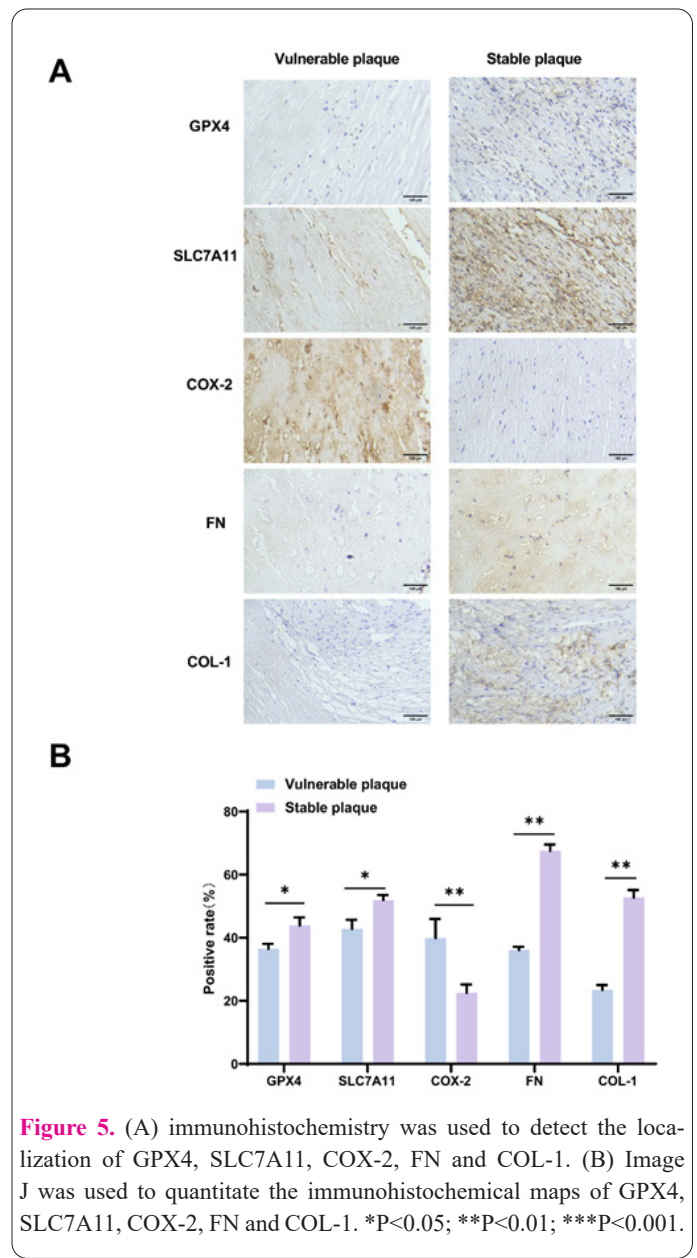
As shown in Figure 5A, immunohistochemical results showed that the tissue localization of GPX4, SLC7A11, FN and COL-1 was significantly denser in stable plaques than in vulnerable plaques. As shown in Figure 5B, quantitative results showed that GPX4 and SLC7A11 had significantly higher protein expression levels in stable plaques than in vulnerable plaques ($P < 0.05$). The protein expression level of COX-2 was significantly lower in stable plaques than in vulnerable plaques ($P < 0.01$). Protein expression of FN ($P < 0.01$) and COL-1 ($P < 0.01$), which are associated with the maintenance of extracellular matrix stability, was significantly higher in stable plaques compared with vulnerable plaques.

Discussion

The pathogenesis of carotid atherosclerosis is complex, and exploring the mechanisms affecting plaque stability is fundamental to the development of drugs for the treatment of atherosclerosis. We compared the degree of ferroptosis in atherosclerotic plaque, demonstrating that reducing ferroptosis could have a stabilizing effect on the plaques. In a previous study, significantly lower levels of GPX4, SLC7A11, and GSH were detected in mouse aortic endothelial cells that underwent ferroptosis compared with those that did not (26). In the present study, a significant reduction in GPX4, SLC7A11, and GSH levels in vulnerable plaques was also demonstrated, suggesting that a higher

degree of ferroptosis progression was occurring in vulnerable plaques. GPX4 is the major phospholipid hydroperoxide (PLOOH)-neutralizing enzyme and it is involved in ferroptosis induced by erastin/RSL3 (27). The GSH pathway has been identified as a key antioxidant defense pathway. The central role of this process is the conversion of GSH to oxidized glutathione (GSSH) by GPX4, which protects cells from iron deposition by limiting cytotoxic lipid peroxidation (28).

Under oxidative stress conditions, SLC7A11 plays a key role in regulating cystine uptake to inhibit oxidative responses and maintain cell survival, and cystine is the rate-limiting precursor of GSH (29). In the present study, the experimental results showed that the expression of GPX4, GSH and SLC7A11 in vulnerable plaques was lower than that in stable plaques, suggesting that vulnerable plaques induced ferroptosis through the GSH/GPX4 pathway. ROS, SOD and MDA are important indicators of ferroptosis, ROS-induced accumulation of lipid peroxides is the ultimate cause of cellular ferroptosis, SOD is an active substance for scavenging oxygen radicals and MDA is the product of lipid peroxidation (30). Iron metabolism imbalance can trigger ferroptosis from multiple pathways, excess Fe^{2+} can promote lipid peroxidation by generating



ROS by the Fenton reaction (31). In this study, concentrations of ROS, MDA, and Fe²⁺ measured by ELISA and flow cytometry were significantly higher in vulnerable plaques than in stable plaques, which exhibited higher levels of oxidative stress. The concentration of SOD was higher in stable plaques than in vulnerable plaques, indicating greater antioxidant capacity in stable plaques.

COX-2 is a key enzyme that catalyzes the synthesis of arachidonic acid into the prostaglandin family, which belongs to the membrane-bound proteins and is encoded by the PTGS2 gene. Some studies have shown that COX-2 expression is increased after induction by pro-inflammatory mediators in pathological states such as inflammation and tumor (32). In this study, the expression of COX-2 was found to be significantly higher in vulnerable plaques than in stable plaques, suggesting that a strong inflammatory response exists in vulnerable plaques. We also explored the expression of genes related to extracellular matrix stability. FN is expressed in the extracellular matrix and plays a role in cell adhesion and maintenance of cell morphology (20), and COL-1 has high tensile strength and constitutes the extracellular matrix network (21). Our results found that the expression of FN-1 and COL-1 in vulnerable plaques was significantly smaller than that in stable plaques, suggesting that instability exists in the extracellular matrix of vulnerable plaques, which is prone to cell detachment, resulting in fragmentation and detachment of plaques, leading to the progression of atherosclerosis. These conclusions are consistent with the pathological results, which showed sparse tissue junctions in the vulnerable plaques, as well as higher levels of inflammatory cell infiltration, more diffuse collagen fibers, and larger particles of lipid droplets.

The results of this study suggest that inhibition of ferroptosis is an important way to stabilize atherosclerotic plaque. The findings of this study provide new ideas about carotid atherosclerosis disease mechanisms and clinical drug targets. Reducing the degree of ferroptosis can attenuate the disease progression and stabilize atherosclerotic plaques. Stabilization of plaque can further reduce the risk of ischemic cerebrovascular disease. The approach of stabilizing the onset and progression of ferroptosis within the carotid plaque has broad research potential. Exploring the relationship between ferroptosis and atherosclerotic plaques will provide a basis for future drug development for the treatment of carotid atherosclerosis.

Ferroptosis is involved in the process of atherosclerotic plaque formation. In advanced atherosclerotic disease, vulnerable plaques have a higher degree of Ferroptosis than stable plaques. The ferroptosis signaling pathway may provide a target for the treatment of atherosclerosis.

Conflict of interests

The authors declared no conflict of interest.

References

1. Emini VB, Perrotta P, De Meyer G, et al. Animal models of atherosclerosis. *Eur J Pharmacol* 2017; 816: 3-13.
2. Moore KJ, Tabas I. Macrophages in the pathogenesis of atherosclerosis. *Cell* 2011; 145(3): 341-355.
3. Roth GA, Johnson C, Abajobir A, et al. Global, Regional, and National Burden of Cardiovascular Diseases for 10 Causes, 1990 to 2015. *J Am Coll Cardiol* 2017; 70(1): 1-25.
4. Lopes BT, Montrezol FT, Silva Terra VD, Medeiros A. A Single Mindfulness-Based Meditation Session Can Produce Reductions in Cardiovascular Risk in Hypertensive Patients: A Pilot Study. *Altern Ther Health M* 2022; 28(2): 18-23.
5. Liu J, Ma C. Current state of cardiovascular research in China. *Nat Rev Cardiol* 2019; 16(10): 575-576.
6. Falk E. Pathogenesis of atherosclerosis. *J Am Coll Cardiol* 2006; 47(8 Suppl): C7-C12.
7. Tabas I, Garcia-Cardena G, Owens GK. Recent insights into the cellular biology of atherosclerosis. *J Cell Biol* 2015; 209(1): 13-22.
8. Halvorsen B, Otterdal K, Dahl TB, et al. Atherosclerotic plaque stability--what determines the fate of a plaque? *Prog Cardiovasc Dis* 2008; 51(3): 183-194.
9. Bonati LH, Nederkoorn PJ. Clinical Perspective of Carotid Plaque Imaging. *Neuroimag Clin N Am* 2016; 26(1): 175-182.
10. Takai H, Uemura J, Yagita Y, et al. Plaque Characteristics of Patients with Symptomatic Mild Carotid Artery Stenosis. *J Stroke Cerebrovasc* 2018; 27(7): 1930-1936.
11. Li J, Wu H, Hang H, et al. Carotid vulnerable plaque coexisting with cerebral small vessel disease and acute ischemic stroke: a Chinese Atherosclerosis Risk Evaluation study. *Eur Radiol* 2022; 32(9): 6080-6089.
12. Jiang X, Stockwell BR, Conrad M. Ferroptosis: mechanisms, biology and role in disease. *Nat Rev Mol Cell Bio* 2021; 22(4): 266-282.
13. Ouyang S, You J, Zhi C, et al. Ferroptosis: the potential value target in atherosclerosis. *Cell Death Dis* 2021; 12(8): 782.
14. Ahluwalia N, Genoux A, Ferrieres J, et al. Iron status is associated with carotid atherosclerotic plaques in middle-aged adults. *J Nutr* 2010; 140(4): 812-816.
15. Li B, Wang C, Lu P, et al. IDH1 Promotes Foam Cell Formation by Aggravating Macrophage Ferroptosis. *Biology-Basel* 2022; 11(10): 1392.
16. Chistiakov DA, Melnichenko AA, Myasoedova VA, Grechko AV, Orekhov AN. Mechanisms of foam cell formation in atherosclerosis. *J Mol Med* 2017; 95(11): 1153-1165.
17. Kloc M, Kubiak JZ, Ghobrial RM. Macrophage-, Dendritic-, Smooth Muscle-, Endothelium-, and Stem Cells-Derived Foam Cells in Atherosclerosis. *Int J Mol Sci* 2022; 23(22): 14154.
18. Gaschler MM, Stockwell BR. Lipid peroxidation in cell death. *Biochem Bioph Res Co* 2017; 482(3): 419-425.
19. Yang WS, Stockwell BR. Ferroptosis: Death by Lipid Peroxidation. *Trends Cell Biol* 2016; 26(3): 165-176.
20. Rajasekaran K, Duraiyaran S, Adefuye M, Manjunatha N, Ganduri V. Kawasaki Disease and Coronary Artery Involvement: A Narrative Review. *Cureus J Med Science* 2022; 14(8): e28358.
21. Latif R, Mumtaz S, Al Sheikh MH, Chathoth S, Al Naimi SN. Effects of Turmeric on Cardiovascular Risk Factors, Mental Health, and Serum Homocysteine in Overweight, Obese Females. *Altern Ther Health M* 2021; 27(114-119).
22. Fic P, Zakrocka I, Kurzepa J, Stepulak A. [Matrix metalloproteinases and atherosclerosis]. *Postep Hig Med Dosw* 2011; 65: 16-27.
23. Little PJ, Chait A, Bobik A. Cellular and cytokine-based inflammatory processes as novel therapeutic targets for the prevention and treatment of atherosclerosis. *Pharmacol Therapeut* 2011; 131(3): 255-268.
24. Stary HC, Chandler AB, Dinsmore RE, et al. A definition of advanced types of atherosclerotic lesions and a histological classification of atherosclerosis. A report from the Committee on Vascular Lesions of the Council on Arteriosclerosis, American Heart Association. *Circulation* 1995; 92(5): 1355-1374.
25. Naghavi M, Libby P, Falk E, et al. From vulnerable plaque to

- vulnerable patient: a call for new definitions and risk assessment strategies: Part I. *Circulation* 2003; 108(14): 1664-1672.
26. Bai T, Li M, Liu Y, Qiao Z, Wang Z. Inhibition of ferroptosis alleviates atherosclerosis through attenuating lipid peroxidation and endothelial dysfunction in mouse aortic endothelial cell. *Free Radical Bio Med* 2020; 160: 92-102.
27. Zhu L, Luo S, Zhu Y, et al. The Emerging Role of Ferroptosis in Various Chronic Liver Diseases: Opportunity or Challenge. *J Inflamm Res* 2023; 16: 381-389.
28. Ursini F, Maiorino M. Lipid peroxidation and ferroptosis: The role of GSH and GPx4. *Free Radical Bio Med* 2020; 152: 175-185.
29. Lee J, Roh JL. SLC7A11 as a Gateway of Metabolic Perturbation and Ferroptosis Vulnerability in Cancer. *Antioxidants-Basel* 2022; 11(12):2444.
30. Fujii J, Homma T, Osaki T. Superoxide Radicals in the Execution of Cell Death. *Antioxidants-Basel* 2022; 11(3): 501.
31. Forcina GC, Dixon SJ. GPX4 at the Crossroads of Lipid Homeostasis and Ferroptosis. *Proteomics* 2019; 19(18): e1800311.
32. Clemente SM, Martinez-Costa OH, Monsalve M, Samhan-Arias AK. Targeting Lipid Peroxidation for Cancer Treatment. *Molecules* 2020; 25(21):5144.